

Synthesis of mesostructured thin films by ionic wind assisted electrostatic spray deposition

Khodadadi, S.; Meesters, G. M H; Biskos, G.

DOI

[10.1016/j.partic.2015.09.006](https://doi.org/10.1016/j.partic.2015.09.006)

Publication date

2016

Document Version

Accepted author manuscript

Published in

Particuology: science and technology of particles

Citation (APA)

Khodadadi, S., Meesters, G. M. H., & Biskos, G. (2016). Synthesis of mesostructured thin films by ionic wind assisted electrostatic spray deposition. *Particuology: science and technology of particles*, 27, 128-132. <https://doi.org/10.1016/j.partic.2015.09.006>

Important note

To cite this publication, please use the final published version (if applicable). Please check the document version above.

Copyright

Other than for strictly personal use, it is not permitted to download, forward or distribute the text or part of it, without the consent of the author(s) and/or copyright holder(s), unless the work is under an open content license such as Creative Commons.

Takedown policy

Please contact us and provide details if you believe this document breaches copyrights. We will remove access to the work immediately and investigate your claim.

Synthesis of mesostructured thin films by ionic wind assisted Electrostatic Spray Deposition

S. Khodadadi¹, G. M. H. Meesters¹, G. Biskos^{1,2,3*}

¹Faculty of Applied Sciences, Delft University of Technology,
Delft 2628-BL, The Netherlands

²Faculty of Civil Engineering and Geosciences, Delft University of Technology,
Delft 2628-CN, The Netherlands

³Energy Environment and Water Research Center, The Cyprus Institute,
Nicosia 1645, Cyprus

Abstract: Thin films produced by Electrostatic Sprayed Deposition (ESD) have nanometer-size structures despite that the size of the initial sprayed droplets is typically a few tens of microns in diameter. This is not only affected by the solvent properties and drying kinetics, but also by Coulomb fission due to the high surface charge density that they built up upon evaporation. Here we modulate the charge density of the droplets by inducing ionic wind along the spray and produce mesoscopic structures. Using WO_3 as an example, we show that the technique provides a practical way to control the morphology of thin films produced by ESD.

Keywords: Electrodynamic atomization, electrospray, aerosols, tungsten oxide, porous thin films

1. Introduction

Applications of thin films span over a wide spectrum ranging from batteries, catalysts, sensors as well as products in medicine (Patil *et al.*, 2009; Garsuch *et al.*, 2010; Qu *et al.*, 2010; Chan and Kwok, 2011; Gurlo, 2011; Isaac *et al.*, 2015). In order to tailor the functional properties of the films to match the requirements of the final products, one needs to have good control over their structure, which in turn depends on the size and morphology of their nanoparticle building blocks. Advances in particle technology have provided a wide range of wet chemistry and gas-phase methods for synthesizing particle building blocks for the fabrication of thin film materials (Kemell, *et al.*, 2005; Biskos *et al.*, 2008; Jaworek and Sobczyk, 2008; Chan and Kwok, 2011). Among these approaches, electrostatic spray deposition (ESD) is a fast and cost-effective method for producing fine particles with narrow size distributions, which in turn can be deposited onto a wide range of substrates in a controlled manner (Jayasinghe *et al.*, 2004).

In ESD, a solution is dispensed into droplets under the influence of electrical forces. Depending on the electric field strength and the properties of the sprayed solution (i.e., surface tension and conductivity), a range of single- and multi-jet modes can be achieved (Jaworek and Krupa, 1999; Yurteri *et al.*, 2010). Since the pioneering work of Rayleigh (1882) on the theory of dispersion of liquids into small charged droplets under the influence of an electrical field, there have been many attempts to model and control the different spraying modes (Hartman *et al.*, 1999; Jaworek and Krupa, 1999; Jayasinghe *et al.*, 2004; Xie *et al.*, 2006; Yurteri *et al.*, 2010).

Most of the modeling and experimental studies have focused on the cone-jet mostly because it yields monodisperse droplets. Even in this ideal mode, an electrospayed charged droplet undergoes Coulomb fission as the liquid evaporates and its surface charge reaches the Rayleigh limit. Coulomb fission causes the charged unstable droplet to explode yielding a number of stable smaller droplets and increasing the polydispersity of the final particles. The charge density of the

constantly evaporating droplet can be reduced by passing the formed droplets (particles) through an ionized environment (Tang and Gomez, 1994, 1995; Chen *et al.*, 1995; Ebeling *et al.*, 2000, 2001; Ijsebaert *et al.*, 2001; Biskos *et al.*, 2005; Laschober *et al.*, 2006).

In this letter we introduce the ionic wind assisted ESD and show its capability to produce thin films of mesoscopic structure. Using WO_3 as a test material we further demonstrate how the structure of the resulting films can be tuned by varying the operating conditions of the process. This builds upon our earlier efforts to control the morphology of thin films produced by ESD in view of making gas sensors (Gaury *et al.*, 2013; 2014).

2. Experimental

The schematic layout of the experimental set up used in the measurements reported in this work is shown in Figure 1. The setup consisted of a syringe pump, an electrospray nozzle (0.25 mm ID and 0.52 mm OD) surrounded by 12 corona needles, a grounded ring and a heated collection plate. The distances between (1) the nozzle and the grounded ring, (2) the corona and the ground electrode, and (3) the nozzle and the heating plate were 6, 2, and 20 mm, respectively. Tungsten precursor solution was prepared as described by Gaury *et al.*(2013): i.e., 5 ml of $\text{W}(\text{pr})_6$ were mixed with 50 ml of 2-propanol under argon atmosphere. The as-prepared precursor solution was then pumped through the electrospray nozzle at flow rates ranging from 0.5 to 10 ml/h. Evaporation of the droplets induced by the elevated temperature of the collection plate and oxidation of tungsten by the presence of oxygen in the air during the ESD, resulted in pure WO_3 nanoparticles and nanostructured film depositions. In an earlier work (Gaury *et al.*, 2013) we have shown that by varying the temperature of the collection plates one can produce dense (at 250 °C), grain-like (275 °C) or highly porous tree-like (300 to 400°C) thin films.

FIGURE 1

To investigate how the ionic wind induced by the corona needles influences the final particle size and morphology of the deposited film, we electrospayed the propanol-tungsten solution in three different modes:

1. the “ V_0 mode” where a constant current was set between the positively charged electrospay nozzle and the grounded heated collection plate, while no voltage was applied to the corona needles,
2. the “ V_{control} mode” where a constant current was set between the positively charged electrospay nozzle and the heated collection plate by controlling the potential on the negatively charged corona needles, and
3. the “ V_{ct} mode” where the maximum achievable negative voltage was applied on the corona needles.

Details of the applied voltage on the electrospay nozzle and the corona needles, and the resulting currents (measured at the electrospay nozzle) are provided in Table 1.

TABLE 1

In all cases, the resulting particles were deposited on Al_2O_3 substrates placed on top of the heating plate that was maintained between 300 and 310 °C in order to produce dense enough films to study by microscopy. The duration of all the depositions was 10 min. The morphological properties of the resulting thin film samples were studied using a Scanning Electron Microscope (SEM; Joel JSM-6010LA). All samples were coated by a thin layer of gold to avoid surface charge disturbances during the measurements.

3. Results and discussion

Figure 2 shows the morphology of the resulting films produced when varying the liquid precursor flow rate and electrical potential applied on the corona needles. When the corona needles are

grounded (i.e., V_0 mode), the resulting structures had a tree-like morphology with primary particles of the order of 100 nm (cf. Fig. 2a and 2b). This observation is in agreement with the structures of the WO_3 films produced by Gaury *et al.* (2013). The tree-like morphology forms because the liquid of the fine droplets undergoing Coulomb fission fully evaporate before reaching the heated collection plate where they preferentially deposit onto already deposited particles. When the flow rate increases to 10 ml/hr, the resulting films transform to a flake-like structure (cf. inset in Fig.2b), mainly because the size of the droplets at the tip of the electro spray and those reaching the substrate are larger.

FIGURE 2

The size of the droplets $d_{droplet}$ at the jet break up point has a power-law dependence to the liquid precursor flow rate. For the widely used cone-jet mode $d_{droplet} \propto (\rho \epsilon_0 Q^4 / I^2)^{\frac{1}{6}}$, where ϵ_0 is the electrical permittivity of vacuum, ρ is the density of the liquid, Q is the flow rate and I is the current of the jet (Hartman *et al.*, 2000). Using these calculations (cf. Gaury *et al.*, 2013, for details), the estimated droplet diameter at the tip of the nozzle ranges from ca. 2 to 10 μm . Considering that the flow rate through the nozzle was from 0.5 to 10 ml/hr the estimated droplet production rate at the tip of the nozzle ranges from ca. 10^9 to 10^{12} #/hr. As the flow rate increases, the probability of the droplets reaching the heated surface before being fully evaporated increases. For the same deposition time, the resulting films will therefore be denser compared to those of the tree-like structures produced at lower flow rates.

Instead of increasing the flow rate, larger droplets reaching the collection plate can result by effectively modulating the charge density of the droplets, thereby prohibiting the Coulomb fission. One way to achieve that is by exposing the particles to ions of the opposite polarity immediately after they are produced by the electro spray. Using the ionic wind assisted

electrospray in V_{control} mode with a 5 and 10 ml/h flow rate yields films with grain sizes of ca. 1 to 2 μm (cf. Fig. 2c and 2d), which are substantially larger compared to those produced by classical ESD. A qualitative description of the process together with detailed SEM images is shown in Fig. 3.

FIGURE 3

The ionic wind also affects the migration time of the droplets from the jet break up point to the heated collecting plate, which also indirectly determines whether the particles reaching the heated collection plate are partially or fully evaporated. Interestingly, when the potential on the corona needles was increased above ca. 3 kV (i.e., at the V_{ct} mode), the electrospray jets started to spin (referred to as the spinning multi-jet mode), spreading the droplets over an area much larger than that of the substrate. As a result, only individual particles were collected onto the substrate as shown in Fig. 2e and 2f, which is not desired for a number of applications where continuous films are required. Estimating the migration time of the droplets from the jet break up point to the heated collection plate is complicated since apart from knowing the convective/turbulent flow pattern, one needs to take into account the strength of the electric field and the changing electrical mobility of the droplets, both of which are difficult to probe or calculate.

Analysis of SEM images showed that the size of the deposited particles in the ionic wind assisted ESD increased from 100-500 nm at a flow rate of 0.5 ml/hr to 1.0-1.5 μm at flow rate of 2.5 ml/h (data not shown). As flow rate increased further to 5-10 ml/hr in V_{ct} mode, agglomerated films with grain sizes of ca. 1-2 μm were deposited on the collection plate along with embryo-like particles having diameters larger than 5 μm (cf. Fig. 4). The shape of the individual particles could be attributed to freezing of a metastable morphology of the drying droplet in a competition between surface tension and electrostatic forces, resulting from passing the particles alternatively through cooler and warmer regions during their deposition.

FIGURE 4

4. Conclusions

In summary, here we introduce the ionic wind assisted EDS method and show that it can be used to produce a range of mesoscopic structures by (1) modulating the surface charge density on the droplets thereby suppressing the Coulomb fission (direct effect), and (2) increasing the residence time of the droplets/particles in the gas phase before deposition on the collection plate (indirect effect). To prove the concept we used a propanol-tungsten precursor solution to synthesize WO_3 particles and structured thin films. The resulting films were highly agglomerated having grain sizes in the range of a few microns, which is substantially larger compared to those produced by classical ESD (i.e., of the order of a 100 nm). By increasing the voltages applied to the corona needles above a certain threshold resulted in a new spraying mode, namely the spinning multi-jet mode, which yields individual particles. Ionic wind assisted ESD therefore provides great opportunities for tailoring the structures of thin films. To control the process for industrial applications, however, further investigation to evaluate the charge state of the droplets and their fission rate will be highly required.

5. ACKNOWLEDGMENTS

The Authors would like to thank the Centre for Concepts in Mechatronics B.V. for providing the test device, J. Gaury for providing the solution sample and J. C. M. Marijnissen for his motivating discussions. SK acknowledges funding from Delft Projectmanagement B.V.-Gilbert project.

Corresponding Author

* E-mail: g.biskos@tudelft.nl; g.biskos@cyi.ac.cy. Tel: +31-1527-88207; +357-22-208-618. Fax: +31-1527-87412; +357-22-208-625.

REFERENCES

- Biskos, G., Reavell, K., & Collings, N. (2005). Electrostatic characterisation of corona-wire aerosol chargers. *J. Electrostat.*, 63, 69-82.
- Biskos, G., Vons, V., Yurteri, C. U., & Schmidt-Ott, A. (2008). Generation and sizing of particles for aerosol-based nanotechnology. *KONA Powder Part J.*, 26, 13-35.
- Chan, H.-K., & Kwok, P. C. L. (2011). Production methods for nanodrug particles using the bottom-up approach. *Adv. Drug Deliv. Rev.*, 63, 406-416.
- Chen, D. R., Pui, D. Y. H., & Kaufman, S. L. (1995). Electro spraying of conducting liquids for monodisperse aerosol generation in the 4 nm to 1.8 μm diameter range. *J. Aerosol Sci.* 26, 963-977.
- Ebeling, D. D., Westphall, M. S., Scalf, M., & Smith, L. M. (2000). Corona discharge in charge reduction electrospray mass spectrometry. *Anal. Chem.*, 72, 5158-5161.
- Ebeling, D. D., Westphall, M. S., Scalf, M., & Smith, L. M. (2001). A cylindrical capacitor ionization source: droplet generation and controlled charge reduction for mass spectrometry. *Rapid Commu. Mass Spectrom.*, 15, 401-405.
- Garsuch, A., Stevens, D. A., Sanderson, R. J., Wang, S., Atanasoski, R. T., Hendricks, S., et al. (2010). Alternative catalyst supports deposited on nanostructured thin films for proton exchange membrane fuel cells. *J. Electrochem. Soc.*, 157, B187-B194.
- Gaury, J., Kelder, E. M., Bychkov, E., & Biskos, G. (2013). Characterization of Nb-doped WO_3 thin films produced by Electrostatic Spray Deposition. *Thin Solid Films*, 534, 32-39.
- Gaury, J., Lafont, U., Bychkov, E., Schmidt-Ott, A., & Biskos, G. (2014). Connectivity enhancement of highly porous WO_3 nanostructured thin films by in situ growth of $\text{K}_{0.33}\text{WO}_3$ nanowires." *Crystengcomm* 16, 1228–1231.

- Gurlo, A. (2011). Nanosensors: towards morphological control of gas sensing activity. SnO₂, In₂O₃, ZnO and WO₃ case studies. *Nanoscale*, 3, 154-165.
- Hartman, R. P. A., Brunner, D. J., Camelot, D. M. A., Marijnissen, J. C. M., & Scarlett, B. (1999). Electrohydrodynamic atomization in the cone-jet mode: Physical modeling of the liquid cone and jet. *J. Aerosol Sci*, 30, 823–824.
- Hartman, R. P. A., Brunner, D. J., Camelot, D. M. A., Marijnissen, J. C. M., & Scarlett, B. (2000). Jet break-up in electrohydrodynamic atomization in the cone-jet mode. *J. Aerosol Sci*, 31, 65-95.
- Ijsebaert, J. C., Geerse, K. B., Marijnissen, J. C. M., Lammers, J. W. J., & Zanen, P. (2001). Electrohydrodynamic atomization of drug solutions for inhalation purposes. *J. Appl. Physiol.*, 91, 2735-2741.
- Isaac, N. A., Ngene, P., Westerwaal, R. J., Gaury, J., Dam, B., Schmidt-Ott, A., & Biskos, G. (2015). Optical hydrogen sensing with nanoparticulate Pd-Au films produced by spark ablation. *Sens. Actuators B: Chemical*, 221, 290–296.
- Jaworek, A., & Krupa, A. (1999). Classification of the modes of EHD spraying. *J. Aerosol Sci.*, 30, 873-893.
- Jaworek, A., & Sobczyk, A. T. (2008). Electro spraying route to nanotechnology: An overview. *J. Electrostat.*, 66, 197-219.
- Jayasinghe, S. N., Edirisinghe, M. J., & Wang, D. Z. (2004). Controlled deposition of nanoparticle clusters by electrohydrodynamic atomization. *Nanotechnology*, 15, 1519-1523.
- Kemell, M., Ritala, M., & Leskelä, M. (2005). Thin film deposition methods for CuInSe₂ solar cells. *Crit. Rev. Solid State Mater. Sci*, 30 1-31.
- Laschober, C., L. Kaufman, S. L., Reischl, G., Allmaier, G., & SzymanskiWladyslaw, W. (2006). Comparison between an unipolar corona charger and a polonium-based bipolar neutralizer

for the Analysis of nanosized particles and biopolymers. *J. Nanosci. Nanotechnol.*, 6, 1474-1481.

Patil, L. A., Shinde, M. D., Bari, A. R., & Deo, V. V. (2009). Highly sensitive and quickly responding ultrasonically sprayed nanostructured SnO₂ thin films for hydrogen gas sensing. *Sens. Actuators B*, 143, 270-278.

Qu, J., Sun, B., Liu, Y., Yang, R., Li, Y., & Li, X. (2010). Improved hydrogen storage properties in Mg-based thin films by tailoring structures. *Int. J. Hydrogen Energy*, 35, 8331-8336.

Rayleigh, L. (1882). On the equilibrium of liquid conducting masses charged with electricity. *Philos. Mag.*, 14, 184-186.

Tang, K., & Gomez, A. (1994). Generation by electrospray of monodisperse water droplets for targeted drug-delivery by inhalation. *J. Aerosol Sci.*, 25, 1237-1249.

Tang, K. Q., & Gomez, A. (1995). Generation of monodisperse water droplets from electrosprays in a corona-assisted cone-jet Mode. *J. Colloid Interface Sci.*, 175, 326-332.

Xie, J., Lim, L. K., Phua, Y., Hua, J., & Wang, C.-H. (2006). Electrohydrodynamic atomization for biodegradable polymeric particle production. *J. Colloid Interface Sci.*, 302, 103-112.

Yurteri, C. U., Hartman, R. P. A., & Marijnissen, J. C. M. (2010). Producing pharmaceutical particles via electrospraying with an emphasis on nano and nano structured particles - A Review. *KONA Powder Part J*, 28, 91-115.

Tables:

Table 1: Summary of operating conditions and observed spraying modes of the ionic wind assisted ESD used in our experiments.

Flow rate (ml/hr)	Nozzle (positive): Voltage (kV) Current (mA)	Corona (negative): Voltage (kV) Current (mA)	Spray mode (naming in figures)
0.5	~ 3.5 kV < 0.01 mA	-	multi-jet (V_0 mode)
	~ 3.5 kV ~ 0.01 mA	~ 2.7 kV ~ 0.01 mA	spinning multi-jet (V_{control} mode)
	~ 3.5 kV ~ 0.2-0.3 mA	~ 3.7 kV ~ 0.03 mA	spinning multi-jet (V_{ct} mode)
2.5	~ 3.5 kV < 0.01	-	multi-jet (V_0 mode)
	~ 3.5 kV ~ 0.02 mA	~ 2.4 kV ~ 0.02 mA	spinning multi-jet (V_{control} mode)
	~ 3.0 kV ~ 0.03-0.04 mA	~ 3.0-3.2 kV ~ 0.03-0.04 mA	spinning multi-jet (V_{ct} mode)
5	~ 4.0 kV < 0.01 mA	-	multi-jet (V_0 mode)
	~ 2.0 kV ~ 0.01 mA	~ 1.9-2.2 kV ~ 0.01 mA	multi-jet (V_{control} mode)
	~ 4.0 kV ~ 0.03 mA	~ 2.9-3.2 kV ~ 0.04-0.04 mA	spinning multi-jet (V_{ct} mode)
10	~ 4.5 kV ~ 0.01 mA	-	multi-jet (V_0 mode)
	~ 4.5 kV ~ 0.01 mA	~ 1.2 kV ~ 0.01 mA	multi-jet (V_{control} mode)
	~ 4.5 kV ~ 0.03-0.04 mA	~ 2.9-3.3 kV ~ 0.03-0.04 mA	spinning multi-jet (V_{ct} mode)

Figure captions

FIGURE 1. Schematic layout of the experimental set up (a), and images of different electrospaying modes (b).

FIGURE 2. SEM images of depositions obtained using flow rates of 5 and 10 ml/h at V_0 mode, (a and b), V_{control} model (c and d) and V_{ct} mode (e and f). The details of the voltages applied on the electrospay nozzle and the corona needles for each case are described in Table 1.

FIRGUE 3. Schematic diagram of the qualitative model (shown on left of SEM images) describing the difference between classical (a) and ionic wind assisted ESD (b). The structure of the resulting WO_3 thin films produced in both cases when a 5 ml/h flow of the propanol-tungsten solution is passed through the nozzle.

Figure 4. SEM images of deposited particles at spinning multi-jet electrospaying mode, as individual particle shape formed by freezing of a metastable morphology of the drying droplet. The dashed circles show the embryo like structure.

Figures:

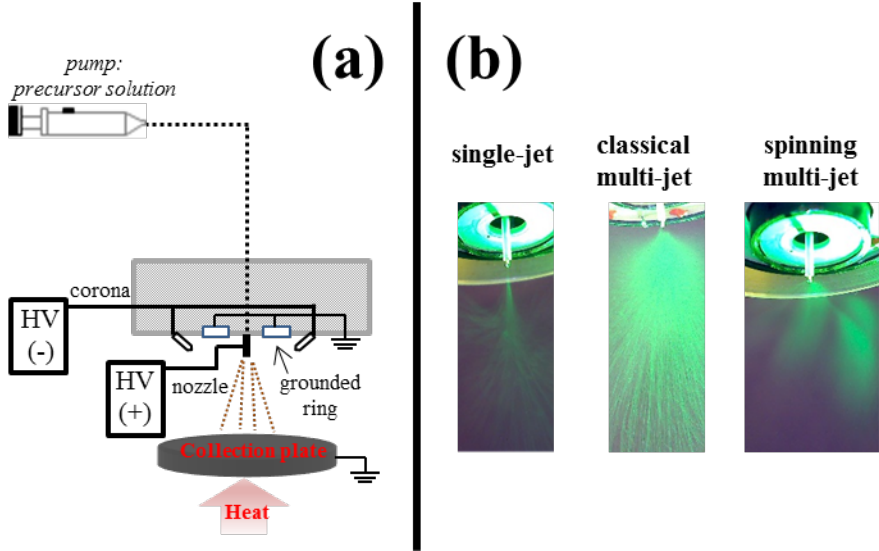


FIGURE 1.

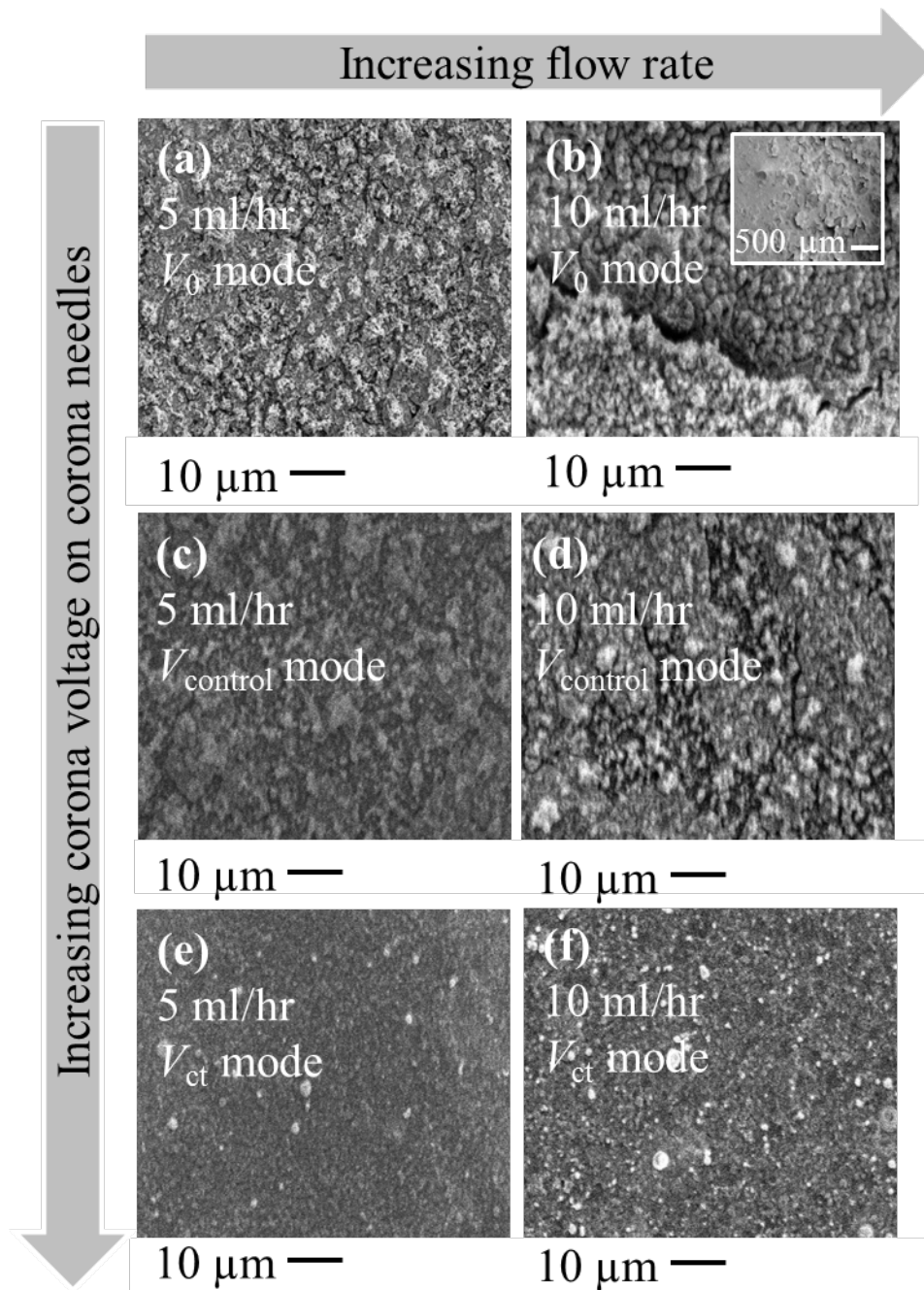
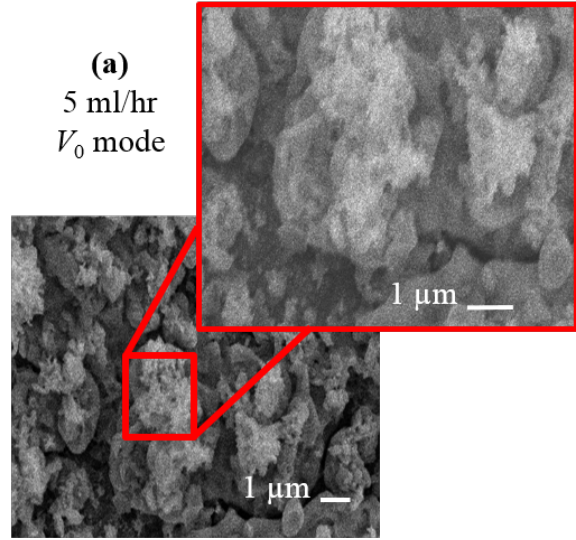
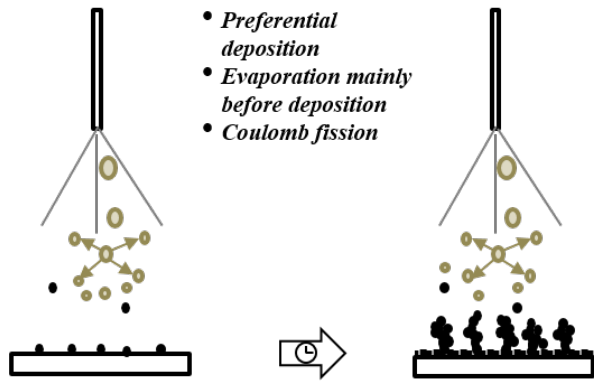
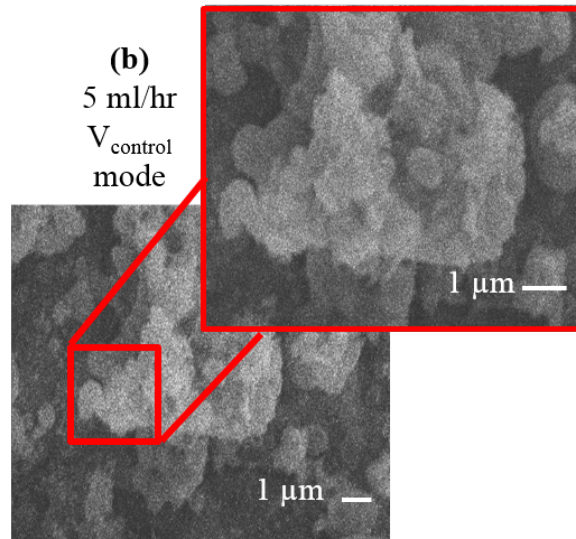
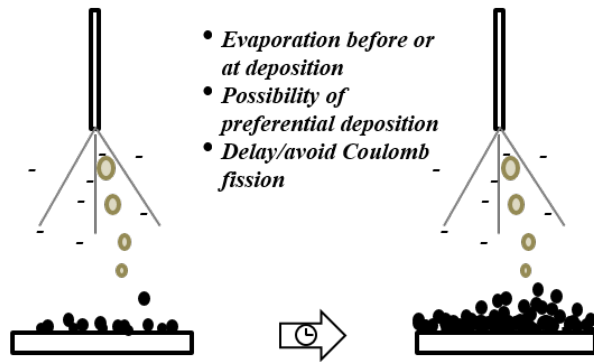


FIGURE 2.

Classical ESD



Ionic wind assisted ESD



FIRGUE 3.

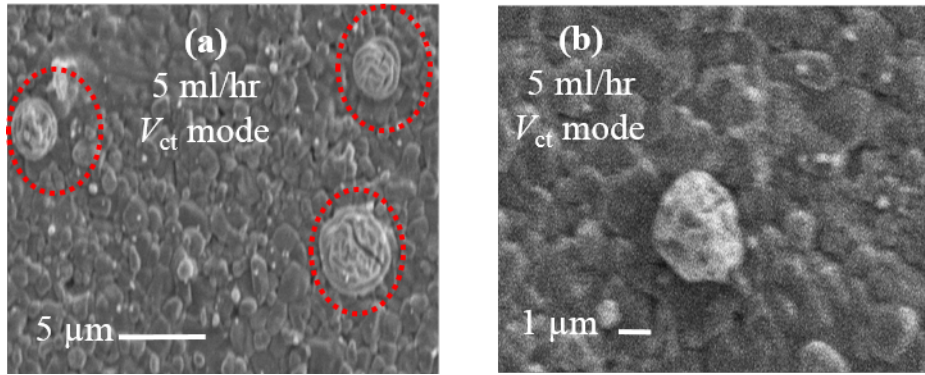


Figure 4.